Forsch Ingenieurwes (2022) 86:513–520
https://doi.org/10.1007/s10010-021-00527-1

ORIGINALARBEITEN/ORIGINALS

Scuffing of cylindrical gears with pitch line velocities up to 100 m/s

J. Vorgerd[1] · P. Tenberge[1] · M. Joop[2]

Received: 29 March 2021 / Accepted: 25 July 2021 / Published online: 15 September 2021

Abstract

Increasing demands on the power density of gearboxes require a precisive gear design regarding common failure mechanism. Particularly in turbo gearboxes with low-viscosity lubricants, the damage mechanism scuffing is relevant. In this paper an innovative test rig for the experimental investigation of scuffing at pitch line velocities up to 100 m/s is presented. The scuffing load capacity depending on the pitch line velocity of two gear design variants running at constant temperatures and lubricant conditions was investigated. Furthermore, the morphology of scuffing was investigated with regard to the damage location and the surface condition. Based on the experimental results, a simulation approach with an accuracy superior to the existing standards for calculating the scuffing load capacity of highspeed gears has been derived.

Untersuchungen zur Fresstragfähigkeit von Stirnradgetrieben bis 100 m/s Umfangsgeschwindigkeit

Zusammenfassung

Steigende Anforderungen an die Leistungsdichte von Getrieben erfordern eine präzise Auslegung gegenüber den gängigen Schadensmechanismen. Besonders durch die Verwendung dünnviskoser Schmierstoffe in Turbogetrieben rückt hierbei der Schadensmechanismus Fressen in den Vordergrund. In dieser Arbeit wird ein innovativer Zahnradverspannungsprüfstand vorgestellt, mit dem die Tragfähigkeit schnelllaufender Stirnradgetriebe mit Umfangsgeschwindigkeiten bis 100 m/s untersucht werden kann. Mit diesem Prüfstand wurden Versuche zur Fresstragfähigkeit in Abhängigkeit der Umfangsgeschwindigkeit mit zwei Geometrievarianten durchgeführt. Die Fressschäden wurden im Hinblick auf die örtliche, topographische Ausprägung mikroskopisch ausgewertet. Basierend auf den experimentellen Ergebnissen wurde ein neuer Berechnungsansatz zur Beschreibung der Fresstragfähigkeit von Turbogetrieben hergeleitet. Verglichen mit den gängigen Berechnungsvorschriften verfügt dieser Ansatz insbesondere im Bereich hoher Umfangsgeschwindigkeiten > 50 m/s über eine deutlich verbesserte Genauigkeit.

Abbreviations

Latin symbols

a [mm]	Center distance
b [mm]	Facewidth
c_p [$\frac{J}{kg \cdot K}$]	Specific heat capacity
d_a [mm]	Tip circle diameter
e_i [–]	Weight parameters
m_n [mm]	Normal modulus
n [rpm]	Rotational speed
p_H [MPa]	Hertzian stress
t_K [s]	Local contact time
v_g [m/s]	Sliding velocity
v_u [m/s]	Tangential velocity (pitch point)
v_Σ [m/s]	Sum velocity
x [–]	Profile shift coefficient
z [–]	Number of teeth
A_K [mm²]	Hertzian contact pattern
C_L [–]	Lubricant factor
C_{Rs} [–]	Roughness factor
E_K [mJ/mm²]	Specific contact energy
E_{spec} [mJ/mm²]	Specific contact energy limit
LS [–]	Load stage
P [kW]	Mechanical power

✉ J. Vorgerd
jaacob.vorgerd@rub.de

[1] Chair of industrial and automotive drivetrains (IFA), Ruhr-University Bochum, Bochum, Germany

[2] Envision Energy CoE GmbH, Dortmund, Germany

P_V [kW]	Power loss
S_B [–]	Scuffing safety factor (flash temperature)
S_E [–]	Scuffing safety factor (energy criterion)
T [Nm]	Torque
$\dot{V}_{oil}$ [l/min]	Oil volume flow

Greek symbols

α_n [°]	Normal pressure angle
β [°]	Helix angle
γ [–]	Heat sharing factor
ε_α [–]	Transverse contact ratio
λ [–]	Specific fluid film thickness
μ_r [–]	Coefficient of friction
ρ_{oil} [kg/dm³]	Density of the lubricant
θ_B [°C]	Maximum contact temperature
θ_S [°C]	Limiting contact temperature
θ_{int} [°C]	Integral tooth flank temperature
θ_{oil} [°C]	Oil injection temperature

Indices

1	Pinion
2	Wheel
n	Index referring to the failure load stage
P	Load dependent
S	Interpolated load stage according to Schlenk
Z	Gear

1 Introduction

Turbo gearboxes almost exclusively use low-viscosity lubricants to reduce load-independent power losses. At the same time, the compromise in the thermal balance leads to allowing the highest possible lubricant temperatures. Consequently, the tooth contacts are tribologically highly stressed and tend to scuff. Scuffed surfaces are heavily roughened with worse frictional properties. This leads to higher power losses and can ultimately cause a gear failure.

The standardized calculation for the scuffing load capacity is given in ISO 6336 [1, 2] and AGMA 925 [3]. However, ISO 6336 states a validation limit of 50 m/s pitch line velocity. AGMA 925 is not explicitly limited, but the experimental data at high pitch line velocities is based on a small number of tests. Especially with respect to the ongoing optimization of turbo gearboxes, these limits in the calculation need to be extended. Therefore, a systematic investigation of the scuffing load capacity at high pitch line velocities is of great interest. This requires special test rig concepts as well as more accurate simulation approaches.

2 Scuffing

Scuffing is a spontaneously occurring surface damage mechanism of tribologically highly stressed cylindrical gears. DIN 3979 [4] differs between cold scuffing, occurring at operating conditions with boundary friction conditions, and warm scuffing. In the case of warm scuffing the elastohydrodynamic lubricant (EHL) film is broken down leading to a local welding of the contacting surfaces, which are immediately torn apart by the rolling kinematic. Consequently, surfaces are locally roughened resulting in increased vibrations and gear friction.

Extensive experimental studies in [5–7] show that scuffing of cylindrical gears can occur if an lubricant depending contact temperature is extended. These experiments cover multiple gear design parameters and sizes. Calculating the contact temperature is done using Blok's theory [8, 9] of a quasi-stationary temperature distribution induced by a moving heat source. Local loads from Hertzian stress, gear friction and sliding heat the contacting surfaces. This approach is used in most calculation models facing scuffing of cylindrical gears. Regarding the load carrying capacity the lubricant itself and its additive content have a superior influence.

The standardized calculation approaches [1, 2] rely on empirical equations which are mainly derived from test results with pitch line velocities below 25 m/s. These approaches indicate a decreasing tendency of the scuffing load capacity with respect to the rotational speed. However, experiments by Borsoff [10], Collenberg [11] and Lechner [5] show a rising scuffing load capacity at high pitch line

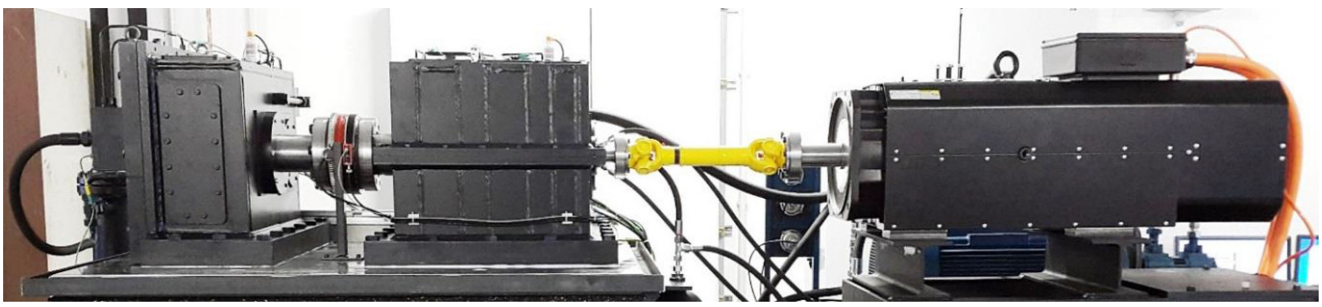

Fig. 1 Picture of the highspeed test rig

velocities after passing a local minimum. These effects are attributed to the EHL conditions and the effects of EP additives in the lubricant. By increasing the pitch line velocity, the EHL film thickness increases and prevents solid contacts.

Experiments in [5, 10, 11] show that suitable calculation models have to consider gear friction and lubricating conditions more precisely. Borsoff [10] and Collenberg [11] recommend scuffing factors depending on the contact time to consider the frictional power density of the contacting surfaces with respect to their sliding paths. Approaches using more tribology based stress factors like the frictional power density are also given by Almen [12] and Dyson [13]. Joop [14] expands these models of the frictional energy and derives a calculation approach that is explicitly valid for high speed gears. The method by Joop will be discussed in this paper.

3 Experimental investigations

3.1 Test rig and test method

The experiments presented in this paper were performed on a highspeed back-to-back test rig shown in Fig. 1. Similar to conventional back-to-back test rigs, a power circuit is set up between a test and a slave gearbox. The shaft system is driven by an electric motor, which only has to feed in power losses. Pitch line velocities up to 100 m/s are possible using this test rig with a center distance of 203.3 mm and a maximum speed at the highspeed shaft of 12,000 rpm.

Table 1 Technical specifications of the highspeed test rig

Denomination	Symbol	Unit	Value
Center distance	a	mm	203.3
Rotational speed pinion shaft	n_1	rpm	Up to 12,000
Torque load at wheel shaft	T_2	Nm	Up to 4000
Circulating mechanical power	P_{mech}	kW	Up to 3300
Lubricant temperature	θ_{oil}	°C	Up to 100

Table 1 shows the relevant technical data of the highspeed test rig.

Due to the requirements of the wide test speed range, the test rig is designed to be torsional stiff to allow a broad operating range without any resonances in the test rig. The mechanism to induce torque is integrated into the slave gearbox. The slave gearbox consists of two separate helical gearsets in V-arrangement whereby the gear wheels can be axially moved by a hydraulic system in relation to the axially fixed pinions. This system allows to induce torque by the gears of the slave gearbox itself without needing an additional rotary actuator. The test rig can be operated at pitch line velocities of 5–25 m/s to calibrate the results with existing test rigs and at pitch line velocities above 30 up to 100 m/s.

Power losses of the test gears are determined with the use of a calorimetric approach by evaluating the temperature increase of the circulating lubricant. The method used is described in [15]. To exclude thermal influences of the bearings, the gear lubrication is thermally insulated by an inner housing. By measuring the oil volume flow, the oil injection temperature and the temperature of the returning oil, total power losses can be calculated with the thermal transport capability of the lubricant under the use of Eq. 1. Load independent and load dependent shares of the total power loss must be separated accordingly.

$$P_V = c_p \cdot \rho_{oil} \cdot \dot{V}_{oil} \cdot \Delta\theta_{oil} \tag{1}$$

The experimental investigations of the scuffing load capacity are carried out with two gear designs (as shown in Table 2). Both variants have a deep tooth form without modifications to the lead or the profile. Experiments using modified gears underlying the same test procedure are described in [16]. The profile shift coefficients are chosen in such a way that balanced sliding velocities are achieved at the start and the end of the path of contact. All gears are made of case-hardened steel 18CrNiMo7-6. The profile is conventionally ground (Ra = 0.3 µm) and the tooth root is untreated.

Apart from the lubrication mode, the test methodology is based on the scuffing test according to ISO 14635-1 [17]

Table 2 Test gear geometry

Denomination	Symbol	Unit	Variant 1	Variant 2
Normal module	m_n	mm	4.5	5.5
Number of teeth	z_1/z_2	–	36/54	30/45
Face width	b_1/b_2	mm	22/20	22/20
Normal pressure angle	α_n	°	20	20
Helix angle	β	°	5	5
Profile shift coefficient	x_1/x_2	–	0.141/–0.135	–0.060/–0.568
Transverse contact ratio	ε_α	–	2.00	2.00
Tip circle diameter	d_{a1}/d_{a2}	mm	174.63/253.45	176.69/253.94

Table 3 Test conditions

Denomination	Symbol	Unit	Variant 1	Variant 2
Pitch line velocity	V_u	m/s	8/20/32/40/58/70/80/90/100	8/20/35/50/70/80/90/100
Hertzian stress (range of the test procedure)	p_H	MPa	146–1,841 (in 12 load stages)	146–1,841 (in 12 load stages)
Test duration	–	min	15	15
Lubricant temperature	θ_{oil}	°C	90	90
Lubricant	–	–	ISO VG 68 (plain mineral oil)	ISO VG 68 (plain mineral oil)

for evaluating the scuffing load carrying capacity of lubricants. Instead of dip lubrication, a temperature-controlled injection lubrication is used. For constant speed and oil conditions, the torque is increased stepwise, until the test gears fail due to scuffing. The nominal Hertzian stress at the pitch point is taken from ISO 14635-1 and the torque is scaled accordingly to account for the larger gears. Before starting the test, the oil system and the test gearbox are heated up to test temperature. Each load stage is then tested for 15 min to establish constant bulk temperatures. Due to scuffing occurring spontaneously, it is important that the test rig is loaded after the nominal speed is set. The loaded gear flanks are inspected with respect to a failure criterion after each load stage. If the damaged flank exceeds 6.25% of the active effective width, the failure criterion is fulfilled. The failure criterium is taken from the ISO 14635-1 to keep the test results comparable with existing standards. All tests were carried out using plain mineral oil of viscosity grade ISO VG 68. The test conditions are given in Table 3.

3.2 Experimental results

Fig. 2 shows results of the scuffing tests performed at different pitch line velocities. In the diagram the torque at the wheel shaft of the respective failure load stage LS_S is plotted as a function of the pitch line velocity. The indiscrete failure load stage LS_S is evaluated in between the adjacent discrete load stages LS_{n-1} and LS_n using a fit method by Schlenk [18]. Both gear variants show a similar behaviour starting with a decrease of the scuffing load capacity in the region of low pitch line velocities. Increasing speed stabilizes the load capacity at 30–60 m/s. At high pitch line velocities above 60 and up to 100 m/s the scuffing load capacity rises to a similar level like in the low-speed regime.

In each load stage temperature conditions of the lubricant can be evaluated for determining the load dependent power losses. Fig. 3 shows the load dependent power losses for the Var. 1 test gears at different speeds. The experiments are proposing a linear correlation between torque and load dependent power losses. An increase of the pitch line velocity also increases the load dependent power losses.

Topography analysis of the test samples with a micro coordinate measurement device shows that the morphology of scuffing changes in respect to the pitch line velocity. The images shown in Fig. 4 are taken from the Var. 1 test pinions. At low pitch line velocities, the tooth tips scuff preferentially, resulting in a heavily roughened surface. Material of the mating gears was transferred to the surface of the pinions. Emerging scuffing marks are orientated in positive sliding direction (Fig. 4a).

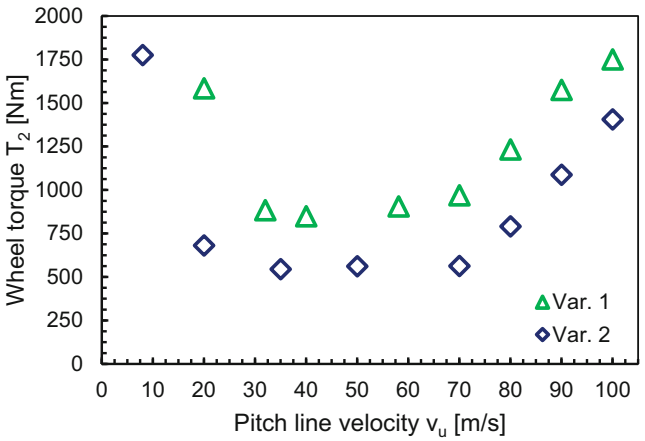

Fig. 2 Scuffing torque at the wheel shaft depending on the test gear variant and test speed

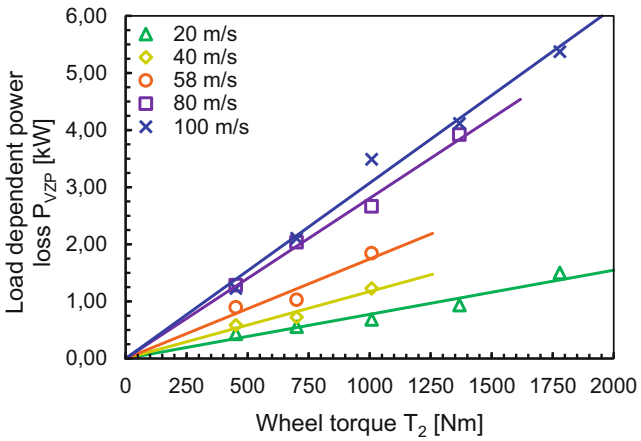

Fig. 3 Load dependent power losses of the Var. 1 test gears at different test speeds

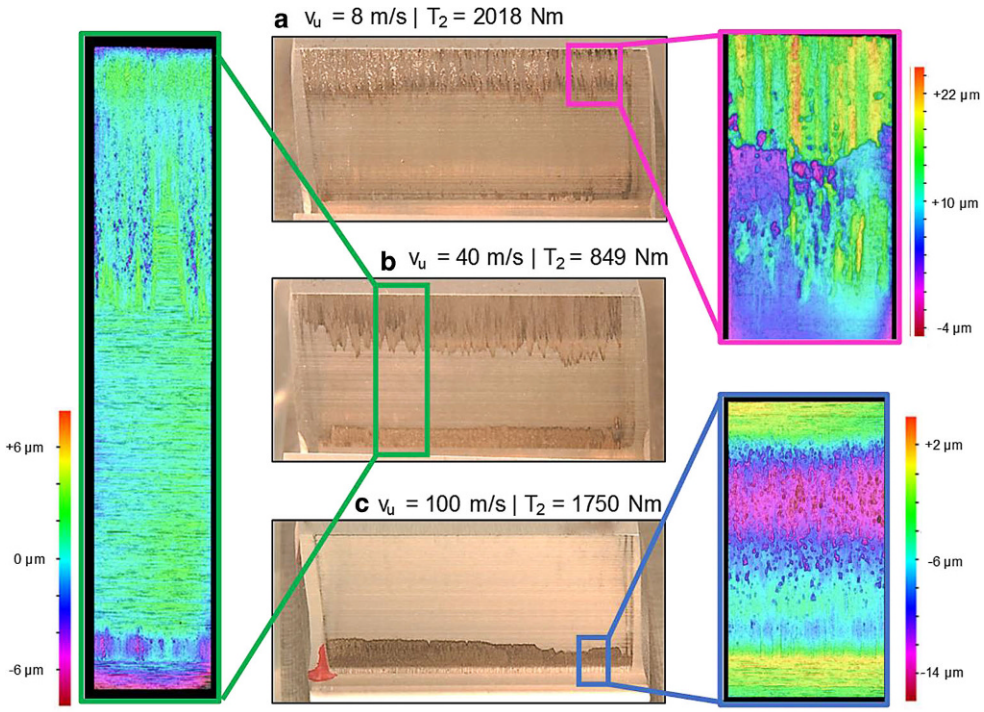

Fig. 4 Pictures and micro coordinate measurements of the pinions scuffed flanks (Var. 1 test samples)

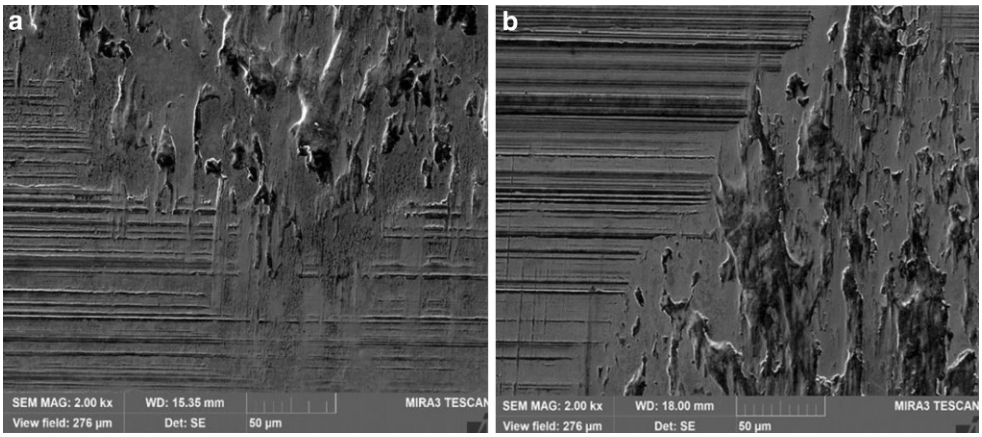

Fig. 5 SEM images of scuffed flank—pinion of Var. 1 test gears at 40 m/s ((**a**)—tooth tip, (**b**)—tooth root)

In the range of moderate pitch line velocities, pinions scuff in areas below and above the pitch point simultaneously. The scuffed region at the tooth tips is worn less than at low speeds. Also, there is no material transfer between the mating gears. In the tooth root region scuffing marks are visible, which are orientated in the direction of negative sliding. There is a material removal of about 6 µm from the unworn surface (Fig. 4b). At high pitch line velocities scuffing is exclusively found at the tooth roots of the pinions. The scuffed patterns are fine and evenly pitted. Scuffing marks are not visible. The material removal amounts to a maximum of 15 µm. The tooth tips of the pinions remain undamaged (Fig. 4c).

Fig. 5 shows scanning electron microscope (SEM) images of the pinions' scuffed surfaces of the Var. 1 sample at 40 m/s pitch line velocity. These images are taken from the transition points from scuffed regions to the unworn flanks of samples with damages at the root and the tip. In both images grinding grooves are clearly visible in the regions without scuffing. The scuffed surfaces show a local material removal in the form of particles which were torn apart due to the rolling motion. Also, grinding grooves are flattened. The emerging scuffing marks are orientated in rolling direction perpendicular to the grinding grooves.

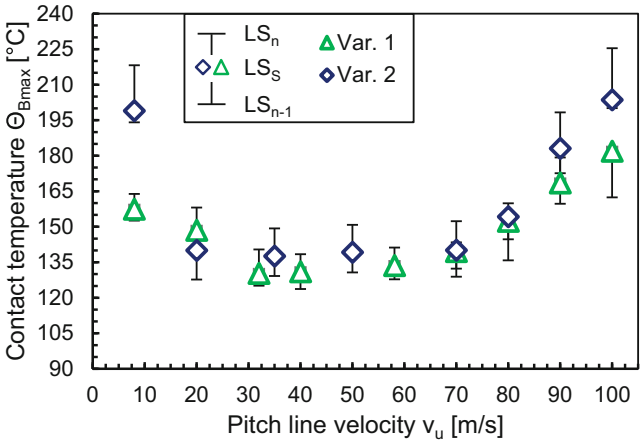

Fig. 6 Max. contact temperature in respect to the pitch line velocity

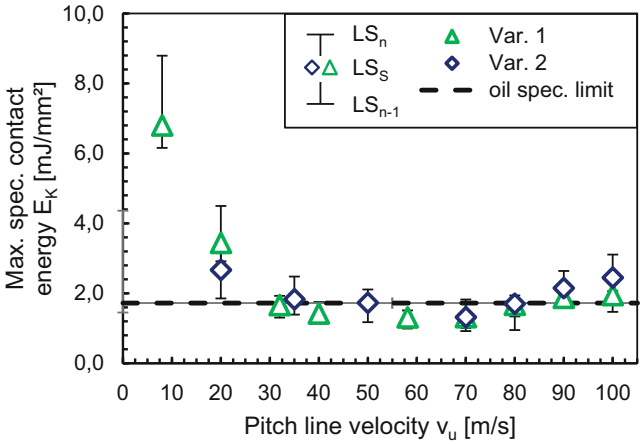

Fig. 7 Max. specific contact energy in respect to the pitch line velocity

4 Simulation approach to calculate scuffing of highspeed gears

The standardized scuffing calculation models, using the flash temperature method shown in Eq. 2, rely on Blok's theory for calculating the maximum contact temperature along the path of contact. The maximum contact temperature Θ_{Bmax} is compared with a lubricant dependent scuffing limit Θ_S. Both temperatures are referred to the lubricant temperature Θ_{oil}. The load distribution assumes a loaded tooth contact without deflections. The calculation of the contact temperature based on Blok's theory assumes a quasi-stationary state. In particular, the unsteady movement of the heat source at the beginning and end of the path of contact as well as the heat conduction in the profile direction cannot be considered.

$$S_B = \frac{\Theta_S - \Theta_{\mathrm{oil}}}{\Theta_{\mathrm{Bmax}} - \Theta_{\mathrm{oil}}} \tag{2}$$

Walkowiak [19] derived an approach for calculating the load distribution of cylindrical gears along the path of contact with respect to local load events at the start and the end of the gear mesh. Along the path of contact, sliding velocities, EHL film thicknesses and contact pressures lead to local gear friction. Joop [14] extended the calculation model by implementing a local-geometric coefficient of friction according to the model given by Klein [20] as shown in Eq. 3. The influence exponents were calibrated based on the measured load-dependent power losses and detailed thermal elastohydrodynamic simulations during FVA project 598 II [16].

$$\mu_r = 0.0232 \cdot {p_H}^{e_1} \cdot {v_\Sigma}^{e_2} \cdot \left|v_g\right|^{e_3} \cdot \lambda^{e_4} \cdot C_L \cdot C_{\mathrm{RS}} \tag{3}$$

In his model Joop enhanced the temperature calculation by implementing a thermal network. The transverse section of the involute is discretized with a network of 400 equidistant nodes in the tooth height direction and 15 nodes in the direction normal to the involute. The elements are thermodynamically bound by the laws of heat conduction. The temporal and spatial integration of the local frictional power in the Hertzian contact patterns is done in 1500 discrete time steps. Except for the friction model the temperature simulation relies completely on physical laws.

Following the flash temperature method, the experimental results are evaluated using the described simulation model to calculate the contact temperatures. Fig. 6 shows the maximum contact temperature Θ_{Bmax} of the corresponding indiscrete failure load stage $\mathrm{LS_S}$ along the pitch line velocity. The error bars illustrate the contact temperatures with the nominal torques of the adjacent discrete load stages LS_{n-1} and $\mathrm{LS_n}$ to cover the maximum spread due to interpolation. Both gear variants scuff at nearly equal contact temperatures. In respect to the pitch line velocity the contact temperature shows a similar tendency as the torque. Considering the maximum contact temperature as a threshold for scuffing extracts the gear geometry, which is why the standardized approaches make use of it. However, since the scuffing limit Θ_S is independent of the pitch line velocity, calculating the scuffing load capacity solely by the flash temperature method is unsuitable for the presented experimental results. Especially in the regime of the raising load capacity at high pitch line velocities a more accurate approach is necessary.

Collenberg [11] already showed that energy criteria assessing gear friction are suitable for calculating scuffing at high pitch line velocities. Joop [14] extends this approach by accumulating the local frictional power losses in the Hertzian contact pattern. The so-called specific contact energy E_K can be understood as a rating for the energetic stress of the tribological contact. Individual sections of the flanks are stressed by frictional power for their correspond-

ing contact time. The calculation of the specific contact energy implies the temporal and spatial integration of the local frictional power. Frictional power losses are distributed on both contact partner using a thermodynamic heat sharing factor γ.

$$E_K = \frac{1}{A_K} \int_{t_K} \gamma \cdot \mu_r \cdot F_N \cdot \left| v_g \right| \, \mathrm{dt} \tag{4}$$

Fig. 7 shows the simulation results at the corresponding failure load stage LS_S of each test point regarding the maximum specific contact energy E_K stressing the pinion flank. Similar to Fig. 6, the sensitivity of the simulation approach is shown by error bars illustrating the maximum contact energies of the adjacent discrete load stages LS_{n-1} and LS_n. Coming from low pitch line velocities the specific contact energy stabilizes on a constant threshold at around 35 m/s. The data points show a good correlation regardless of the gear design. Based on these test results a specific contact energy threshold for plain mineral oil at 90 °C injection temperature of $E_{spec} = 1.7\,\mathrm{mJ/mm^2}$ can be derived. This threshold allows to estimate scuffing of cylindrical gears running at pitch line velocities higher than 35 m/s according to Eq. 5.

$$S_E = \frac{E_{spec}}{E_K} \tag{5}$$

5 Conclusion

In this paper, a test rig concept was presented which can be used to perform scuffing tests of cylindrical gears running at high speeds with pitch line velocities of up to 100 m/s. In addition, experimental results from FVA research project 598 II were presented regarding the scuffing load capacity as a function of the pitch line velocity. The experiments showed a good correlation to the findings of Borsoff [10], Collenberg [11] and Lechner [5] and demonstrated that scuffing and gear friction must be considered coherently. Topography analysis of the scuffed flanks showed a different morphology in respect to the pitch line velocity. Based on the experimental results, a new approach for calculating the local scuffing load capacity at high pitch line velocities was derived. This approach uses an oil dependent specific contact energy threshold for estimating the scuffing load capacity. Particularly for gears running at high pitch line velocities, where the standardized calculations are not valid anymore, this approach exhibits good accuracy. The presented results can be transferred to optimize the power density of turbo gearboxes by a more accurate prediction of scuffing. In further research work, the influences of the lubricant temperature, additives and viscosity need to be investigated to extend the limits of the derived calculation approach.

Funding This publication uses results from FVA project 598 II "örtliche Fresstragfähigkeit" that has been funded by the German Federal Ministry for Economic Affairs and Energy. The authors would like to thank Forschungsvereinigung Antriebstechnik for the founding.

Funding Open Access funding enabled and organized by Projekt DEAL.

References

1. ISO 6336-20 (2017) Calculation of load capacity of spur and helical gears—Part 20: Calculation of scuffing load—Flash temperature method
2. ISO 6336-21 (2017) Calculation of load capacity of spur and helical gears—Part 21: Calculation of scuffing load—Integral temperature method
3. AGMA 925-A03 (2003) Effect of lubrication on gear surface distress
4. DIN 3979 (1979) Zahnschäden an Zahnradgetrieben
5. Lechner G (1966) Die Freßlastgrenze bei Stirnrädern aus Stahl. Dissertation, Technische Universität München
6. Michaelis K (1987) Die Integraltemperatur zur Beurteilung der Fresstragfähigkeit von Stirnradgetrieben. Dissertation Technische Universität München
7. Hepermann P (2013) Untersuchungen zur Fresstragfähigkeit von Groß-, Schräg- und Hochverzahnungen. Dissertation, Ruhr-Universität Bochum
8. Blok H (1937) Measurement of temperature flashes on gear teeth under extreme pressure conditions. Proc Gen Disc Lubric 2:14–20
9. Blok H (1937) Theoretical study of temperature rise at surfaces of actual contact under oiliness lubricating conditions. Proc Gen Disc Lubric 2:222–235
10. Borsoff VN, Godet MR (1963) A scoring factor for gears. ASLE Trans 2:147–153
11. Collenberg HF (1991) Untersuchungen zur Fresstragfähigkeit schnelllaufender Stirnradgetriebe. Dissertation, Technische Universität München
12. Almen JO (1948) Surface deterioration of gear teeth. In: Conference on Mechanical Wear, pp 229–238
13. Dyson A (1975) Scuffing—A review. Tribol Int 8:77–87
14. Joop M (2018) Die Fresstragfähigkeit von Stirnrädern bei hohen Umfangsgeschwindigkeiten bis 100 m/s". Dissertation, Ruhr-Universität Bochum
15. Imdahl MJ (1998) Hochgenaue Wirkungsgradbestimmung an Getrieben unter praxisnahen Betriebsbedingungen. Dissertation, RWTH-Aachen

16. Joop M, Ittenson H (2018) Örtliche Fresstragfähigkeit. Abschlussbericht zu Forschungsvorhaben FVA, vol 598 II
17. DIN ISO 14635 (2006) Zahnräder, FZG-Prüfverfahren Teil 1 – FZG-Prüfverfahren A/8,3/90 zur Bestimmung der relativen Fresstragfähigkeit von Schmierölen
18. Schlenk L (1995) Untersuchungen zur Fresstragfähigkeit von Großzahnrädern. Dissertation, Technische Universität München
19. Walkowiak M (2013) Örtliche Belastungen und Verschleißsimulation in den Zahneingriffen profilkorrigierter gerad- und schrägverzahnter Stirnräder zwischen Einfederungsbeginn und Ausfederungsende. Dissertation, Ruhr-Universität Bochum
20. Klein M (2012) Zur Fresstragfähigkeit von Kegelrad- und Hypoidgetrieben. Dissertation, Technische Universität München